1   Electronic Supporting Information

2   **A Closer Look at the Development and Performance of Organic/Inorganic Membranes Using 2,4,6-**

3   **tris[3(triethoxysilyl)-1-propoxyl]-1,3,5-triazine (TTESPT)**

4   *Suhaina M. Ibrahim,[a,b] Rong Xu,[c] Hiroki Nagasawa,[a] Akinobu Naka,[e] Joji Ohshita,[d] Tomohisa Yoshioka,[a]*

5   *Masakoto Kanezashi,[a]* and *Toshinori Tsuru[a]**

6   [a]Department of Chemical Engineering, Hiroshima University, 1-4-1 Kagamiyama, Higashihiroshima, 739-8527, Japan

7   [b]Advanced Material Research Centre (AMREC), SIRIM Berhad, Lot 34, Jalan Hi-Tech 2/3, Kulim Hi-Tech Park, 09000

8   Kulim, Kedah, Malaysia

9   [c]School of Petrochemical Engineering, Changzhou University, Changzhou, 213164, China

10   [d]Department of Applied Chemistry, Hiroshima University, 1-4-1 Kagamiyama, Higashihiroshima, 739-8527, Japan

11   [e]Department of Life Science, Kurashiki University of Science and the Arts, 2640 Nishinoura, Tsurajima, Kurashiki, Okayama 712-

12   8505, Japan

13

14   **Electronic Supporting Information-1 (ESI-1)**

15   *1.1 Synthesis of 2,4,6-tris[3(triethoxysilyl)-1-propoxyl]-1,3,5-triazine (TTESPT)*

16   TTESPT was synthesized in a (30 mL) two-necked flask equipped with a stirrer and a reflux condenser, into which

17   was placed (4.40 g, 17.7 mmol) of 2,4,6-tris(allyloxy)-1,3,5-triazine and (10.40 g, 63.3 mmol) of triethoxysilane in

18   (10 mL) of toluene. Two drops of (0.1 M) H_2PtCl_6 in *i*PrOH were added, and the mixture was heated to reflux for 4

19   hours. Excess reactant and the solvent were removed under vacuum to give a colorless liquid (12.08 g). All reactions

20   were performed under an atmosphere of dry nitrogen. Figure S1 is a schematic diagram of the synthesis of 2,4,6-

21   tris[3(triethoxysilyl)-1-propoxyl]-1,3,5-triazine (TTESPT)

22

23

24
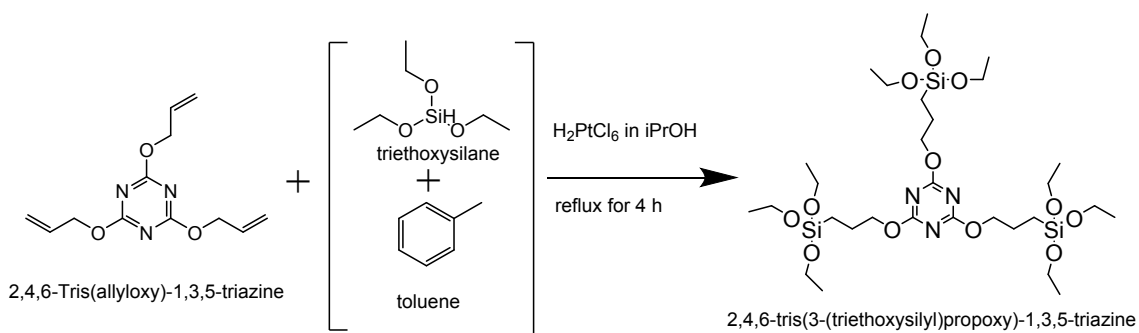
25   **Figure S1** Schematic diagram of the synthesis of 2,4,6-tris[3(triethoxysilyl)-1-propoxyl]-1,3,5-triazine (TTESPT)

26

27   Anal. Calcd and NMR spectra for $C_{30}H_{63}N_3O_{12}Si_3$ (TTESPT)[1a,b] are shown as below (Figure S2):

28   ^{1}H NMR (δ CDCl$_3$) 0.69 (m, 6H, CH$_2$Si) 1.18 (t, 27H, CH$_3$, J = 7.0 Hz), 1.82-1.92 (m, 6H, CH$_2$), 3.78 (q, 18H, CH$_2$O,

29   J = 7.0 Hz), 4.28-4.36 (m, 6H, CH$_2$O);

30   ^{13}C NMR (δCDCl$_3$) 6.40 (CH$_2$Si), 18.20 (CH$_3$), 22.18 (CH$_2$), 58.34 (OCH$_2$), 70.26 (OCH$_2$), 173.02 (triazine carbon).

31

32
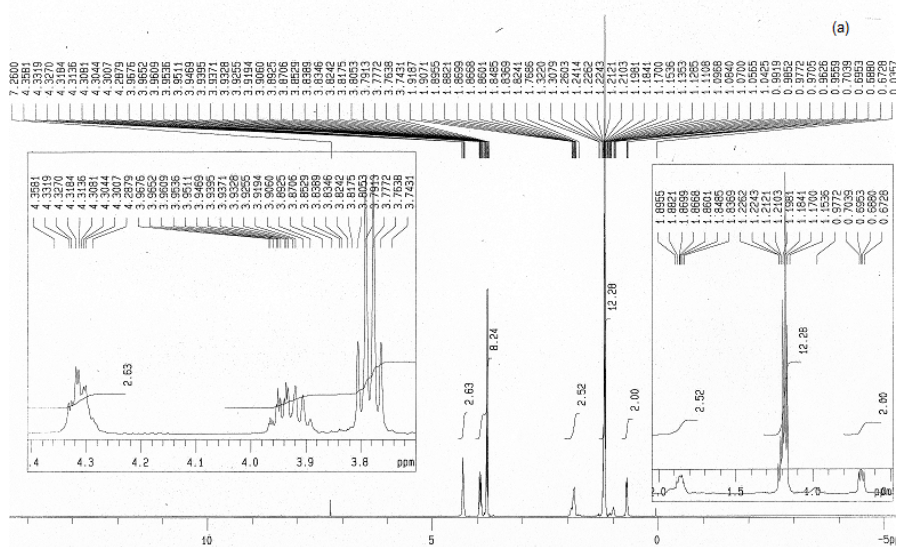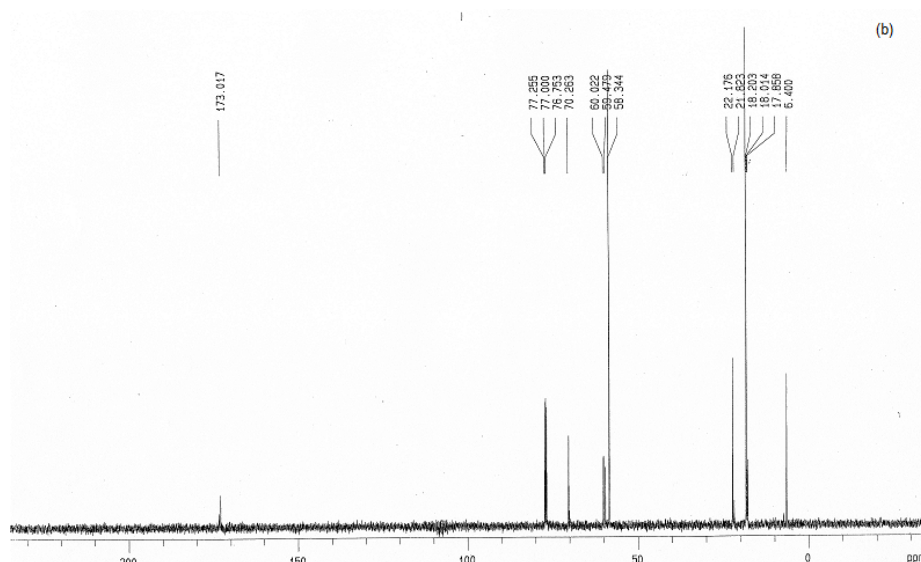
Figure S2 NMR spectra of 2,4,6-tris[3(triethoxysilyl)-1-propyl]-1,3,5-triazine $C_{30}H_{63}N_3O_{12}Si_3$ (TTESPT) solution

(a)^{1}H NMR and (b) ^{13}C NMR

1.2. Preparation of a TTESPT-silica derived membrane

A TTESPT-derived silica solution was prepared using hydrochloric acid as a catalyst. First, TTESPT as a silica precursor was homogeneously dissolved in an ethanol solution. A mixture of water and hydrochloric acid were then added dropwise to the solution under vigorous stirring, resulting in a final solution with molar ratios of TTESPT/H_2O/acid = (1/240/0.2). Then, the solution was kept in a closed system under continuous stirring at 25 °C for 6 h to form silica sols. TEOS, and BTESE-derived silica solutions were prepared for comparison, and the details of the preparation procedure can be found elsewhere.[2-4] Porous α-alumina tubes (porosity: 50%, average pore size: 1 μm, outside diameter: 10 mm) were used as the supports for TTESPT-derived silica membranes. α-Alumina particles (average particle diameter: 0.2, 1.9 μm) were coated on the outer surface of a porous support using silica-zirconia

45 colloidal sol as the binder, and the support was fired at 550 °C for 30 min to make the surface smooth. These

46 procedures were repeated several times to cover large pores that might have resulted in pinholes in the final

47 membrane. Then, a SiO_2–ZrO_2 (Si/Zr = 1/1) solution diluted to about (0.5 wt%) was coated on the substrate to form

48 an intermediate layer with pore sizes of several nm, followed by calcination at 550 °C for about 30 min. Finally, the

49 TTESPT-derived silica layer was fabricated by coating a TTESPT solution, followed by drying and calcination at

50 200, 300 and 400 °C under nitrogen for 30 min.

51

52 *1.3. Characterization of TTESPT-silica derived membrane*

53 ^{1}H NMR and ^{13}C NMR spectra were recorded using a JNM–LA500 spectrometer. Thermogravimetric analysis (TG)

54 was performed to investigate the decomposition behavior of the organic groups in the silica matrix at temperatures

55 ranging from 100 to 800 °C with a heating rate of 10 °C min^{-1} in a Helium flow of 300 ml min^{-1} using a

56 Thermogravimetric Mass Spectrometer (TGA-DTA-PIMS 410/S, Rigaku, Japan).   The TTESPT-derived film coated

57 on the KBr plate was fired between 200 and 550 °C under an N_2 atmosphere, and was characterized by in situ Fourier

58 transform infrared (FTIR) spectroscopy (FTIR-JASCO, Japan). The morphology of TTESPT membranes were

59 examined by using a Hitachi S-48000 scanning electron microscope (SEM). A N_2 adsorption isotherm was carried

60 out at 77 K to study the micropore structures of the silica gels. Prior to the measurement, all the silica gel samples

61 were evacuated at 150 °C for 12 h. The measurements were carried out using BELMAX (BEL JAPAN INC., Japan).

62

63 *1.4. Single gas permeation measurement*

64 Gas permeation tests were performed at temperatures ranging from 200 to 50 °C using a single component of He, H_2,

65 CO_2, N_2, CH_4, C_3H_8, and SF_6 before and after the coating process as shown in Figure S3. The permeation stream was

66 maintained at atmospheric pressure, and the pressure drop through the membranes was maintained at 1 bar. Prior to

67 the measurement, all membranes were outgassed in a He flow of 50 ml min^{-1} at 200 °C for 8 to 12 h to remove any

68 water that possibly absorbed through the membranes.

69

70

71   1. Gas cylinder

72   2. Pressure regulator

73   3. Pressure gauge

74   4. Membrane

75   5. Stop valve

76   6. Soap film meter

77   7. Thermocouple

78   8. Heater
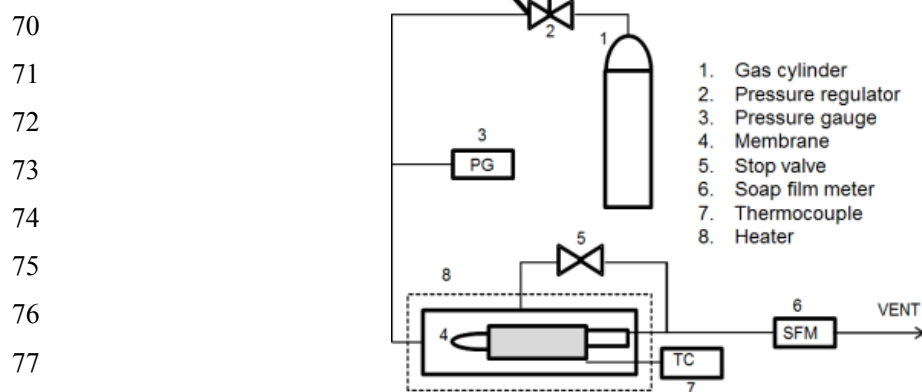
79 **Figure S3** Schematic diagram of the experimental apparatus for single gas permeation measurement

80

81 **Electronic Supporting Information-2 (ESI-2)**

82 Figure S4 shows the SEM images of the surfaces, (a) and (c), and cross-sections, (b) and (d), of TTESPT membranes

83 calcined at 200 and 400 °C under N_2 environment at magnification of 10,000 and 2,000, respectively. As shown in

84 Figures 4 (a) and (c), almost no change occurred to the membrane top surface areas. On the other hand, a very thin

85 layer of TTESPT was successfully coated on the top of SiO_2-ZrO_2 intermediate–alumina particle layer from the cross

86 section shown in Figures 4 (b) and (d).
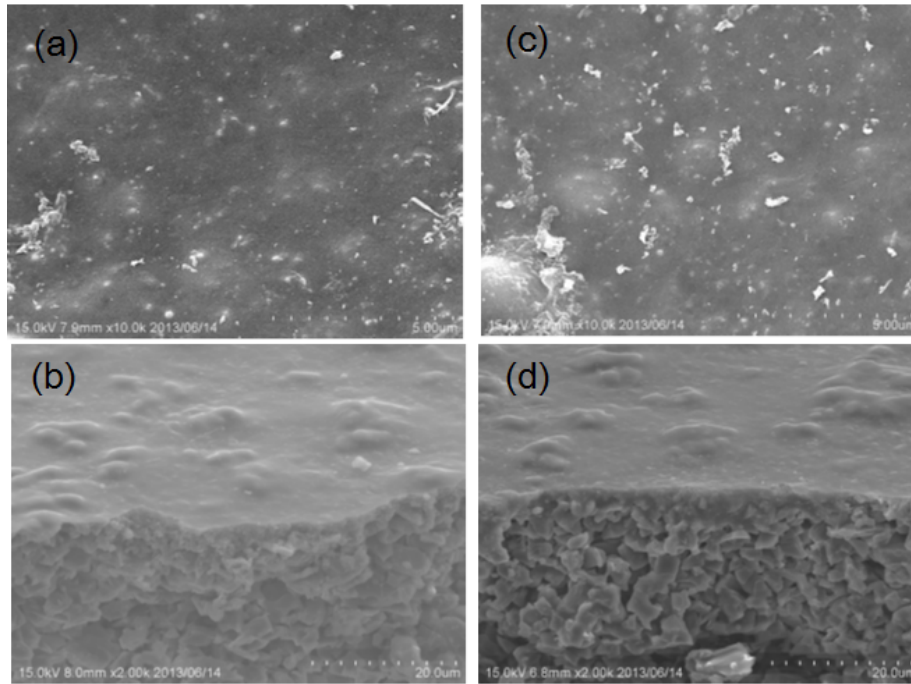
87

88 **Figure S4** SEM images of the surface and cross sections of TTESPT membranes calcined at 200 °C (a and b); 400 °C

89 (c and d) under N_2 environment

90

91 **Electronic Supporting Information-3 (ESI-3)**

92 *2.1 Relationship between temperature dependence of single-gas permeances and quantitave pore size*

93 *measurement (template technique)*

94 Figure S5 shows the gas permeance and selectivity properties for TTESPT-derived silica membranes calcined at 200,

95 300 and 400 °C at a permeation temperature of 200 °C. As shown, as the calcination temperature was increased from

96 200 to 400 °C, and the H_2 permeance increased from 0.93×10^{-6} to 2.39×10^{-6} mol/(m^2 s Pa), while the H_2/N_2 and

97 H_2/CH_4 selectivity decreased from 22 to 7 and 22 to 5, respectively. Calcination at high temperatures clearly showed

98 a different tendency from that observed for the TEOS-derived silica membrane. deVos *et al.*[5-6] reported a decrease in

99 H_2 permeance from 2×10^{-6} to 5×10^{-7} mol/(m^2 s Pa) by calcined TEOS-derived silica membranes at   400

100 to 600 °C, and an increase in H_2/CH_4 selectivity of from 560 to 4,000. The change in the gas permeation properties of

101 TEOS membranes at different calcination temperatures might have resulted from densification, which caused a

102 decrease in the amount of terminal hydroxyl groups at the internal surface of the silica.[5-6] However, in our case, an

103 opposite phenomenon was seen. This phenomenon was known as the template method. Figure S6 shows the

104 schematic images of the formation of TTESPT-silica pore networks via the template method. Obviously, this method

105 can be used in order to tune the pore size of TTESPT-silica derived membrane.
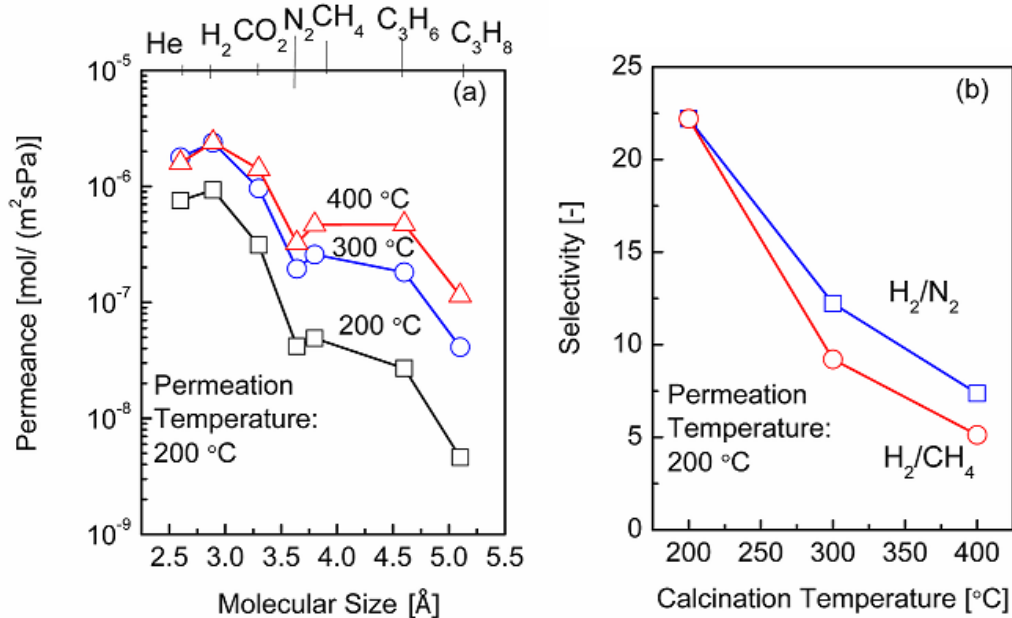
106

107 **Figure S5** (a) Gas permeance and (b) selectivity properties for TTESPT-derived silica membranes calcined at

108 different temperatures of 200, 300 and 400 °C under a N_2 atmosphere at permeation temperature 200 °C

109
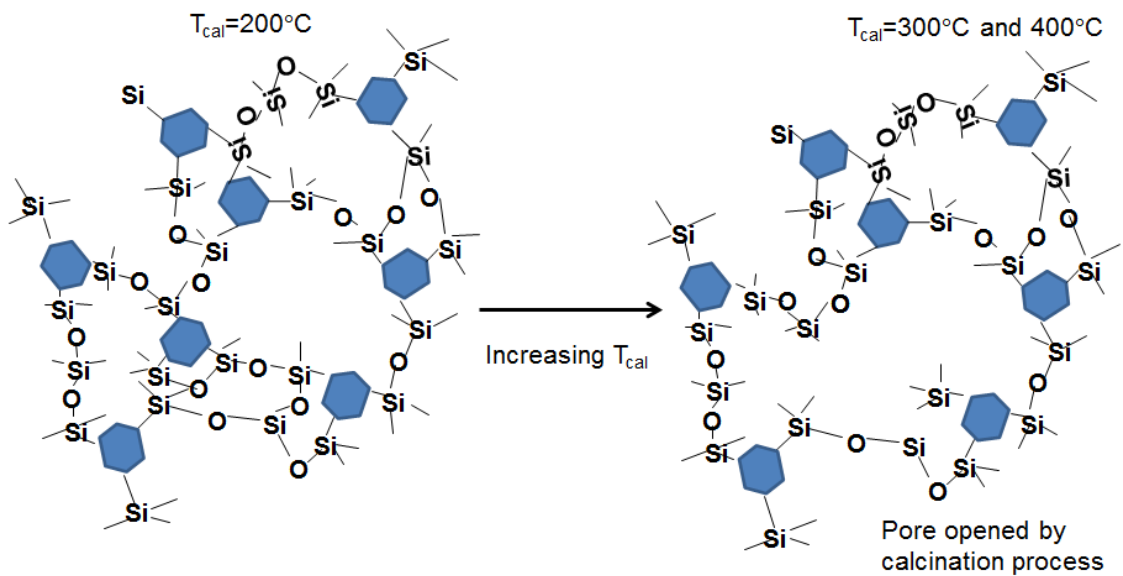
110

111 **Figure S6** Schematic structure of a pore network of TTESPT via the template method.

112

113

114 In order to quatitatively evaluate the pore size of these membranes, a normalized Knudsen-based permeance (NKP)

115 method was applied.[7] This NKP method is based on the modified gas translation (GT) model that was derived by

116 modifying the original GT model proposed by Xiao and Wei[8] and by Shelekhin et al.[9] for the determination of

117 membrane pore sizes of less than 1 nm. As mentioned by Lee et al.,[9] NKP is the permeance ratio of the ith component

118 (P_i) to that predicted from the jth component based on the Knudsen diffusion mechanism, $P_j = \sqrt{M_j/M_i}$ where

119 helium, the smallest molecule, is used as a reference (jth component). NKP can be expressed by Eq. (1).

120
$$NKP = \frac{P_i}{P_{He}\sqrt{M_{He}/M_i}}$$
(1)

121 NKP is equal to 1 for all gases; Knudsen diffusion is the dominant mechanism. In the original GT as shown in Eq. (2),

122 the molecular size is not explicitly incorporated based on the assumption that the size of the gas is small enough.

123
$$P_i = d_p \rho_{g,i} \sqrt{\frac{8}{\pi M_i RT}} \frac{\varepsilon_i}{\tau_i L_i} \exp\left(-\frac{E_{p,i}}{RT}\right)$$
(2)

124 The diffusion distance of the ith component, d_p, is assumed to be (d_p-$d_{k,i}$) for the ith component (molecular size: $d_{k,i}$)

125 due to the steric hindrance, the permeance, P_i, through microporous inorganic membranes (membrane porosity, ε;

126 pore diameter, d_p; tortuosity, τ, thickness, L) can be formulated as the modified GT-model in Eq. (3) by using the

127 molecular weight of the permeating component, M, gas constant, R, and the temperature, T. The probability of the ith

128 component, $\rho_{g,i}$, corresponds to the geometrical probability; that is, the product of the effective area for permeation,

129 $(d_p-d_{k,i})^2/d_p^2$. [7-9]

130
$$P_i = \frac{(d_p - d_{k,i})}{3}\left(\frac{(d_p - d_{k,i})^2}{d_p^2}\right)\sqrt{\frac{8}{\pi M_i RT}}\frac{\varepsilon_i}{\tau_i L_i}exp\left(\frac{E_{p,i}}{RT}\right)$$
(3)

131 Therefore, by inserting Eq. (3) into Eq. (1), and an assumption of the negligible difference of the activation energy of

132 permeation, NKP can be formulated as Eq. (4).

133
$$NKP = \frac{(d_p - d_{k,i})^3}{(d_p - d_{k,He})^3}$$
(4)

134 The pore size of TTESPT-derived silica membranes obtained via the NKP method also shifted from 0.5 to 0.8 nm

135 when the calcination temperature was increased from 200 to 400 °C (Figure S7). This can be ascribed to the partial

136 removal of triazine-based linking units as confirmed by FTIR spectra. A similar trend has also been reported for

137 MTES, TEDMDS and MTES and TEOS-derived silica membranes.[4,7] An enhancement of gas permeance was☐

138 observed after the membranes were calcined at a higher temperature under environments of N_2 and air.

139
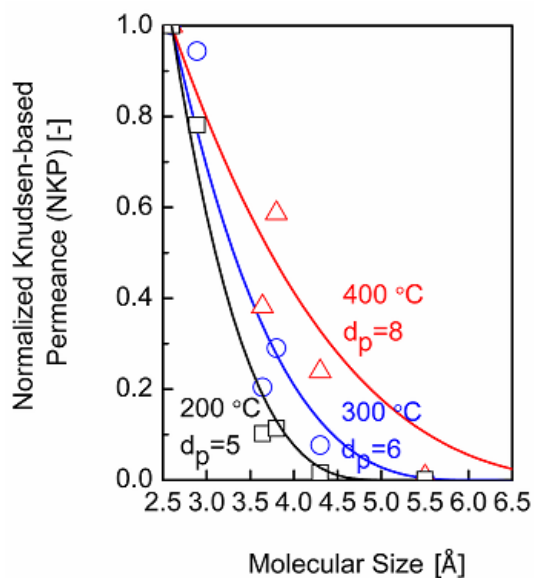
Figure S7   Normalized Knudsen-based permeance as a function of molecular size at a permeation temperature of 200 °C; points are experimental and curves are calculated for TTESPT-derived silica membranes calcined at different temperatures of 200, 300 and 400 °C.

References

1   (a) J.L. Speier, *Adv. Organomet. Chem.* 1979, **17**, 407.

     (b) J. L. Speier, J. A. Webster, G.H. Bernes, *J. Am. Chem. Soc.* 1957, **79**, 974.

2   M. Kanezashi, A. Yamamoto, T. Yoshioka, T. Tsuru, *AlChE J.* 2010, **56**,1204.

3   M. Kanezashi, K. Yada, T. Yoshioka, T. Tsuru, *J. Membr. Sci.* 2010, **348**, 310.

4   G. Li, M. Kanezashi, T. Tsuru, *J. Membr. Sci*. 2011,**379**, 287.

5   R.M. de Vos, H. Verweij, *Sci.* 1998, **279**, 1710.

6   R.M. de Vos, H. Verweij, *J. Membr. Sci*. 1998, **143**, 37.

7   H. R. Lee, M. Kanezashi, Y. Shimomura, T. Yoshioka, T. Tsuru, *AIChE J.* 2011, **57**, 2755.

8   Xiao, J. Wei. *Chem. Eng. Sci.*1992. **47**, 1123

9   A.B. Shelekhin, A.G. Dixon, Y.H. Ma. *AIChE J.*1995**, 41,** 58